Nanoscale

Accepted Manuscript

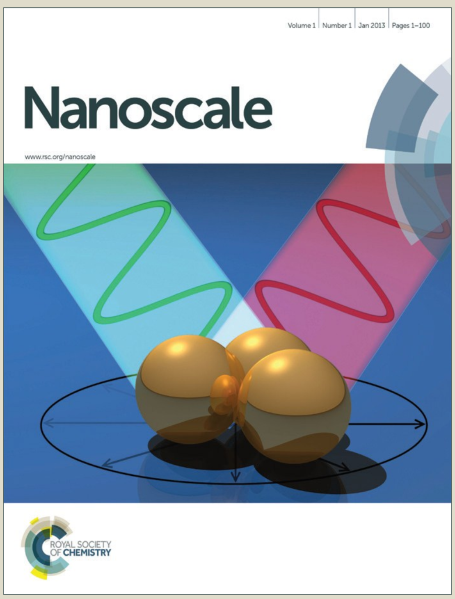

Nanoscale

ARTICLE

Floating compression of Ag nanowire networks for effective strain release of stretchable transparent electrodes

Received 00th January 20xx,
Accepted 00th January 20xx

DOI: 10.1039/x0xx00000x

www.rsc.org/

Jun Beom Pyo,‡[a] Byoung Soo Kim,‡[ab] Hyunchul Park,[c] Tae Ann Kim,[a] Chong Min Koo,[c] Jonghwi Lee,[b] Jeong Gon Son,[a] Sang-Soo Lee,*[ad] and Jong Hyuk Park*[a]

Manipulating the configuration of Ag nanowire (NW) networks has been pursued to enhance the performance of stretchable transparent electrodes. However, it has remained challenging due to the high Young's modulus and low yield strain of Ag NWs, which lead to their mechanical failure when subjected to structural deformation. We demonstrate that floating a Ag NW network on water and subsequent in-plane compression allows convenient development of a wavy configuration in the Ag NW network, which can release the applied strain. Greatly enhanced electromechanical stability of Ag NW networks can be achieved due to the wavy configuration, while the NW networks maintain desirable optical and electrical properties. Moreover, the produced NW networks can be transferred to a variety of substrates, offering flexibility for device fabrication. The Ag NW networks with wavy configurations are used as compliant electrodes for dielectric elastomer actuators. It demonstrates their promising potential to provide improved performance for soft electronic devices.

Introduction

Stretchable transparent electrodes are an essential component for the development of many soft electronic devices[1–3] including flexible touch screens,[4,5] deformable solar cells,[6,7] and epidermal sensors.[8,9] These electrodes need to satisfy the following qualities: (i) electrical conductivity, (ii) optical transparency, and (iii) mechanical stretchability. Transparent conducting oxides (TCOs) have been the material most widely used for transparent electrodes in hard electronics, as they offer strong performance in electrical and optical properties. However, the brittle nature of TCOs fails to meet the third qualification, mechanical stretchability, to be applied in soft electronic devices. Therefore, searching novel materials that fulfil all three attributes is needed to produce stretchable transparent electrodes.

An extensive range of materials has been investigated as potential candidates for stretchable transparent electrodes, including conductive polymers,[10–12] carbon-based materials,[13–15] and metal nanowires (NWs).[16–23] Previous studies have shown that it is challenging for conductive polymers and carbon-based materials to attain the desired levels of electrical conductivity and optical transparency at the same time.[10–12,24–26] Metal NWs, especially Ag NWs, have been considered promising because electrodes incorporating NW networks can achieve both high conductivity and transparency simultaneously.[27–29] Unfortunately, however, Ag NW itself has exhibited restrictions in its stretchability because the yield strain of individual Ag NWs is only ~1.5% in the uniaxial direction.[30]

One strategy to address this issue is to bypass the poor stretchability of Ag NWs via manipulating the structure of the NW network to endure mechanical stress when stretched. Three-dimensional (3D) Ag NW networks with a microporous structure have been introduced, which were fabricated by using ice or polymer templates.[31,32] Deformation of these 3D networks alleviated the stress applied to the Ag NWs. In addition, wrinkled substrates incorporating Ag NW networks have been employed for stretchable electrodes.[19,33] The wrinkles flattened, which mitigated the stress applied to the Ag NWs. However, despite such progress being achieved, stretchable transparent electrodes would still benefit from further improvement of the procedures. For example, 3D NW networks needed to overcome the low transparency problem due to light scattering for the porous structure. Wrinkles on substrates also caused large surface roughness, restricting applicability.

Developing a wavy configuration in Ag NW networks can be a feasible way to avoid these problems and maintain enhanced stretchability. Wavy-configured networks can release the applied strain by straightening NWs, resulting in

[a.] Photo-Electronic Hybrids Research Center, Korea Institute of Science and Technology, Seoul 136-791, Republic of Korea.
[b.] Department of Chemical Engineering and Materials Science, Chung-Ang University, Seoul 156-756, Republic of Korea.
[c.] Center for Materials Architecturing, Korea Institute of Science and Technology, Seoul 136-791, Republic of Korea.
[d.] KU-KIST Graduate School of Converging Science and Technology, Korea University, Seoul 136-701, Republic of Korea.
† Electronic Supplementary Information (ESI) available: A supporting document with additional technical details is included as a separate PDF file. See DOI: 10.1039/x0xx00000x
‡ Both authors contributed equally to this work.

reduced mechanical stress when stretched. Indeed, for networks composed of silicon NWs or carbon nanotubes, their wavy configuration was helpful in reinforcing the stretchability.[34–36] Moreover, the issues of light scattering and surface roughness can be prevented because a wavy-configured NW network has a two-dimensional form and stands on flat substrates. However, few studies have been reported on wavy configurations of Ag NW networks. It is presumably because the high Young's modulus and low yield strain of Ag NWs easily lead to mechanical failure of the Ag NWs themselves or their networks when force is applied to manipulate the configuration.[30,37,38] Consequently, a simple and compatible approach that provides Ag NW networks with a wavy configuration is necessary to produce effective stretchable transparent electrodes.

Here, we present a facile method to develop wavy configurations in Ag NW networks. The wavy configuration of Ag NWs can be obtained by floating the Ag NWs on water and subsequent in-plane compression. These NW networks show greatly enhanced electromechanical stability due to the wavy configuration. Moreover, the NW network produced can be transferred to a variety of substrates, thus providing flexibility for device fabrication. It is further demonstrated that the wavy-configured Ag NW networks function properly as compliant electrodes for dielectric elastomer actuators. Thus, this approach can be a useful tool to fabricate stretchable transparent electrodes for various soft electronic devices.

Results and discussion

A wavy configuration can be introduced into Ag NW networks by applying pressure parallel to the plane of the NW networks, which is similar to compressing a fishnet. However, the high Young's modulus and low yield strain of Ag NWs cause mechanical failure of the NWs when compressed.[30,37,38] In addition, a NW network in the form of a thin film is vulnerable to large external forces. To develop a wavy configuration without breaking the NWs or their network, the smallest possible force needs to be applied. It should also be noted that since a NW network must be supported by a specific substrate, the force applied to manipulate the configuration increases due to friction between the NW network and the substrate. Conventionally, most substrates for NW networks have been solid materials, causing high friction and thus inevitable damage to the NW network during the application of force. For this reason, developing wavy configurations in NW networks has remained challenging. To address this problem, we suggest a smart solution: substitution of the substrate from solid to liquid, that is suspending a NW network on liquid and compressing it.

Fig. 1 describes the method for preparing Ag NW networks with wavy configurations. The procedure begins by filtering a solution of dispersed Ag NWs, which have an average diameter of ~115 nm and an average length of ~40 µm. The Ag NW network is peeled off the filter by dipping it gently into water;

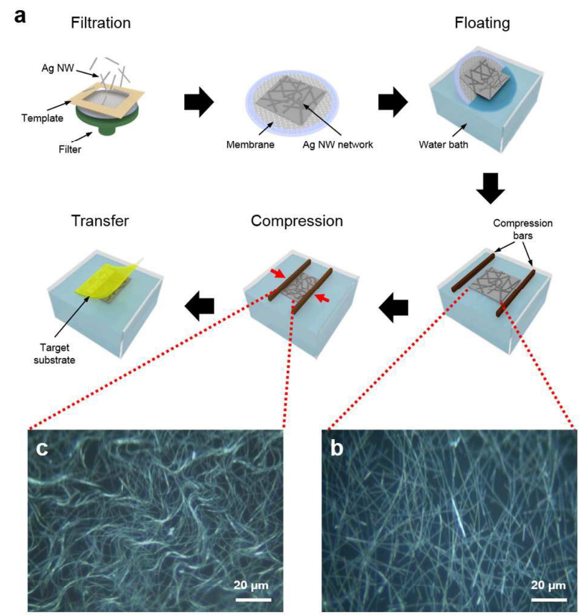

Fig. 1 (a) Schematic for the preparation of Ag NW networks with wavy configurations. Optical microscope images of Ag NW networks floated on water (b) before and (c) after compression.

the Ag NW network then floats on the water surface due to the surface tension of the water supporting the network. The surface tension of an air-water interface, in particular, is helpful to prevent wrinkles in suspended NW networks.[39,40] As shown in Fig. S1†, neither the structural change nor realignment of NWs was yet observed during this floating process. Compression is a key process that initiates the structural transformation in NW networks. By the compression, NWs in the networks are bent and slipped simultaneously. However, the bending of NWs is dominant because the binding between NWs at the junction points of the networks restricts the slipping of NWs. It is noteworthy that the area density of NWs in the networks needs to be controlled. Applying the floating compression method to very sparse or dense NW networks was challenging (Fig. S2†).

After compressing the network uniaxially, a wavy configuration develops in the NW network successfully. This approach is not limited to a specific kind of NWs. As shown in Fig. S3†, the networks of NWs with different dimensions can also be transformed into wavy structure. The resulting products are easily transferred to target substrates by contact from the air side of the water-air interface. Transfer via the water side of the interface, by dipping a substrate into the water and scooping out the network, is best avoided, as such a process may rupture the NW network.[40,41] These procedures allow the stress applied to the network to be minimized, resulting in successful fabrication and transfer of wavy-configured NW networks.

To control the morphology of a Ag NW network, the degree of compression (Δ) applied to the network was

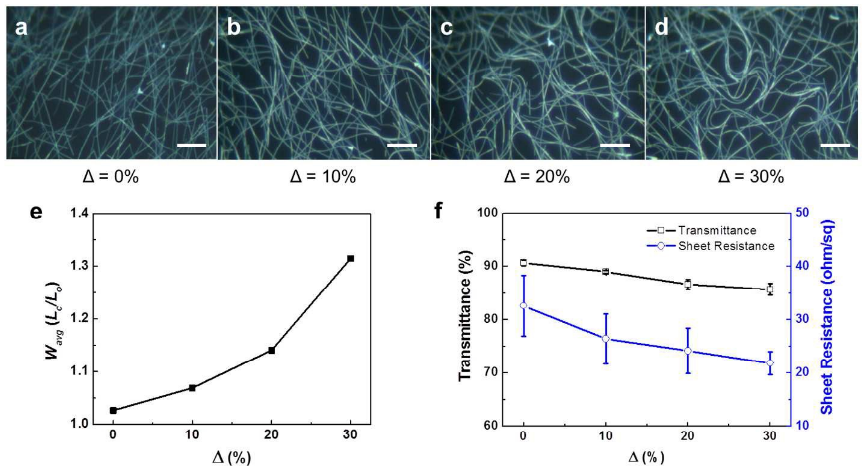

Fig. 2 Optical microscope images of Ag NW networks with controlled degrees of compression (Δ) of (a) 0%, (b) 10%, (c) 20%, and (d) 30%. The scale bars included in the images are 10 µm. (e) Average degree of waviness of NW networks as a function of the degree of compression. (f) Transmittance at 550 nm and sheet resistance of NW networks as a function of the degree of compression. These properties were characterized after transferring the network to PDMS substrates.

regulated. The value of Δ was determined based on the ratio of the compressed length of the network to its initial length (25 mm). As described in Fig. 2a-d, an experimental Ag NW network exhibited a wavier configuration as Δ was increased. The individual NWs in the network had smoothly curved shapes without fractures even for a Δ value of 30 % (Fig. 2d). This is because the low friction between the floating NWs and the water allows free movement that distributes the compressive force evenly rather than concentrating the stress on certain points of the NWs. However, the maximum value of Δ was limited to 30%; above 30%, macroscopic deformation (rupturing and folding) of the NW network was observed. Therefore, we used Δ values of 10%, 20%, and 30% (Fig. S4†). In order to quantify the waviness of NW networks with different Δ values, the degree of waviness (*W*) was defined as follows.

$$W = L_c / L_0 \qquad (1)$$

where L_c and L_0 are the contour length and the end-to-end distance of individual NWs, respectively; a detailed description of the measurement of L_c and L_o is provided in the Supplementary Information (Fig. S5†).

After transferring the compressed NW network to polydimethylsiloxane (PDMS) substrates, the W values for individual NWs in networks with different Δ values were observed. The average degree of waviness (W_{avg}) of each NW network was determined by averaging the *W* values of 50 NWs. Fig. 2e shows the relationship between W_{avg} and Δ, indicating the W_{avg} proportional to Δ. The W_{avg} for NW networks with Δ values of 0%, 10%, 20%, and 30% were 1.03, 1.07, 1.14, and 1.31, respectively. The optical and electrical properties of the NW networks deposited on PDMS substrates were characterized as presented in Fig. 2f. Their transmittance spectra in the wavelength range from 350 to 800 nm are provided in Fig. S6†. The transmittance and sheet resistance exhibited conspicuous propensities: decreasing transmittance and sheet resistance with increasing Δ. These results are reasonable, because increasing Δ leads to the increased population of NWs per unit area, which implies relatively large conductive portions and small vacant portions in the network. In particular, it was observed that applying even small compression reduced the resistance of the NW network significantly. A pristine NW network (Δ = 0%) had sheet resistance of 32.6 ohm/sq and transmittance of 90.7% at 550 nm. However, with a Δ value of 10%, the sheet resistance decreased by 19 % (~26.4 ohm/sq), while the transmittance remained at an equivalent level (~89.0% at 550 nm). This is because the compression process improves the electrical contact between the NWs. As shown in Fig. 2a-d, the compression process induced microscopic overlapping and bundling of NWs, increasing the contact area between the NWs.

The PDMS substrates incorporating the NW networks showed desirable optical and electrical properties which were comparable to those of commercial TCO substrates (transmittance: 80-97% at 550 nm and sheet resistance: 5-100 ohm/sq).[42] Therefore, the produced substrates should function as effective transparent electrodes. Followed by this step, their resistance variation due to mechanical strain was investigated to examine the performance as stretchable electrodes. Changes in sheet resistance as a function of strain were expressed as the ratio of the resistance value (R) at a given strain to the initial value (R_0) at zero strain. Strain (ε) was uniaxially applied to the substrates in the same direction as the compression. It was defined by the ratio of the extended length to the length of the initial substrate without stretching (20 mm).

Regardless of Δ, the sheet resistance of all substrates increased as mechanical strain increased. However, such increase in the resistance was reduced by the introduction of wavy configurations in the NW networks, offering enhanced electromechanical stability as stretchable electrodes. As shown in Fig. 3a, the change in the resistance ratio became smaller as the waviness of NWs increased. Under ε of 30%, the R/R_0 value of substrates with an uncompressed NW network (Δ = 0%) increased to 7.40, while those of substrates with Δ values of 10%, 20%, and 30% were 4.60, 3.20 and 2.22, respectively. These dramatic differences in resistance ratios due to the configuration of the NW network were seldom seen in past studies, indicating the significance of the wavy configuration. Since NW networks with wavy configurations have more NWs per unit area than uncompressed ones, the changes in resistance might originate from this rather than the configuration. To verify this, the same measurements were conducted using uncompressed networks with controlled population of NWs; we assumed that the optical transmittance of networks is governed by the population of NWs, and thus the transmittance of the uncompressed networks was adjusted to be identical to that of a wavy-configured network with a Δ value of 30% (85.7% at 550 nm). Even though the increase in the resistance of the uncompressed network was reduced with higher population of NWs, the R/R_0 value (4.75 at ε of 30%) was much inferior to that of the wavy-configured network (Fig. S7a†).

Reliable electrical resistivity after repeated stretching is also necessary for stretchable electrodes. A uniaxial ε of 10% was applied to the substrates, which were then contracted to 0% multiple times. The R/R_0 values of NW networks for various numbers of cycles were shown in Fig. 3b. The R/R_0 values of the NW networks with Δ values of 0% and 30% increased as the number of cycles increased, presumably because some NWs became disconnected when stretched. However, the R/R_0 value was much smaller for a NW network with a wavy configuration (1.51 at 50 cycles) than for one without (3.53 at 50 cycles). In addition, the former almost stabilized after around 50 cycles, whereas the latter continued to increase. Thus, the wavy configuration of the NW network provided stable recovery of electrical conductivity and improved reliability as a stretchable electrode. The influence of NW population was also examined for this measurement (Fig. S7b†), which confirmed that the stable recovery of electrical conductivity was due to the wavy configuration rather than differences in NW population. These Ag NW electrodes were connected in an electric circuit with a light-emitting diode (LED) lamp to visually compare their electromechanical stability. An LED lamp glowed when the wavy-configured NW network (Δ = 30%) was stretched to 100% while the lamp was off when the uncompressed electrode was stretched to only 50% as shown in Fig. 3c-d.

The morphology of Ag NW networks during stretching was observed in real time using an optical microscope. A Ag NW network prepared by compressing with a Δ value of 30% was stretched uniaxially with ε values of 0%, 10%, 20%, and 30% whose morphologies were presented in Fig. S8†. Before applying ε, the W_{avg} value for the network was about 1.32, which was consistent with the value shown in Fig. 2e. As ε increased, the NWs exhibited a straightened configuration and thus W_{avg} decreased to 1.06 at ε of 30%. This indicates that wavy configurations in NW networks allow release of applied strain via straightening of the NWs, preventing a failure of the NWs themselves or their networks. Consequently, developing wavy configurations in NW networks is an effective strategy to improve the electromechanical stability of NW network-based

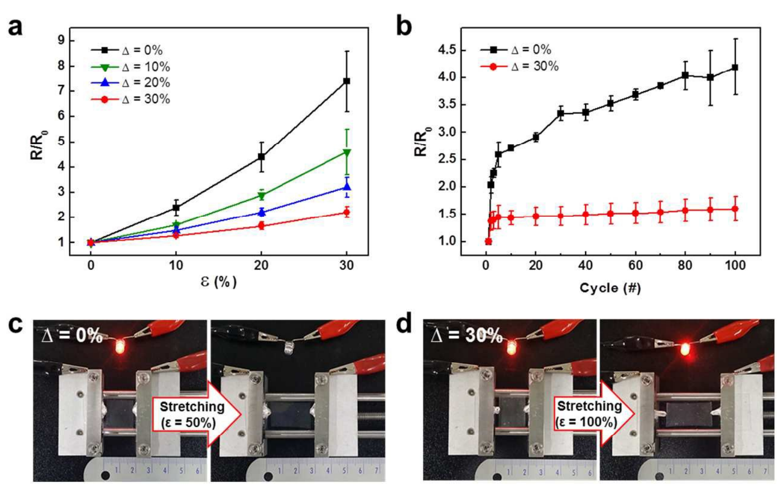

Fig. 3 Electromechanical stability of Ag NW networks prepared using different degrees of compression (Δ), transferred onto PDMS substrates. (a) Variation in sheet resistance as a function of strain (Ɛ). The strain was uniaxially applied to the substrates in the same direction as the compression. Some error bars are not shown because they are smaller than the size of the data points. (b) Variation in sheet resistance as a function of cycle number. A 10% strain was repeatedly applied to the network. (c) An LED lamp is turned off when the uncompressed network (Δ = 0%) is stretched to 50%. (d) An LED lamp is glowing when the wavy-configured network (Δ = 30%) is stretched to 100%.

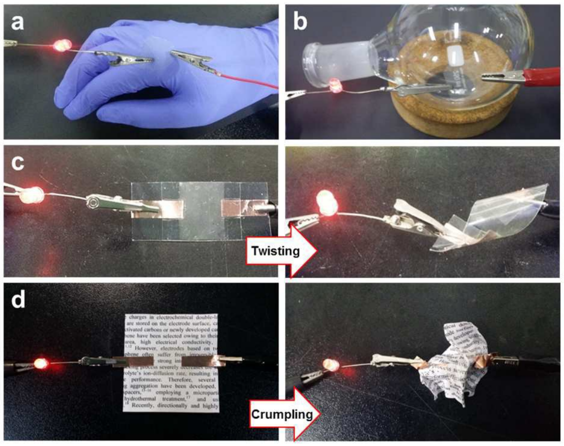

Fig. 4 Ag NW networks transferred onto (a) a nitrile rubber glove, (b) a glass flask, (c) a PET film, and (d) a sheet of paper. On all substrates including a twisted PET film and crumpled paper, the transferred networks functioned properly as an electrically conductive medium for lighting an LED lamp.

electrodes.

Our approach has an additional benefit that the NW networks produced can easily be transferred to a variety of substrates, thereby providing enhanced flexibility in device fabrication. Previously, transfer of NW networks has been possible by stamping, but only with soft and sticky substrates such as PDMS.[17,43,44] In addition, NW networks have been created on hard substrates via bar-coating or spray-coating of NW suspensions, but it is difficult to manipulate the configuration of the NWs using these methods.[4,5,18,28,45] In contrast, a wavy-configured NW network created when floating on water is, in principle, transferrable to any desired substrate regardless of its surface state or shape. As shown in Fig. 4a-b, Ag NW networks were successfully deposited on a hydrophobic surface of nitrile rubber as well as a hydrophilic glass surface. Moreover, even though these substrates were not at all flat, the resulting networks worked as an electrically conductive medium. We also examined the deformability of these networks on substrates. A polyethylene terephthalate (PET) film with a Ag NW network was twisted and paper with a Ag NW network was crumpled (Fig. 4c-d); nevertheless, neither network was collapsed or detached from the substrates, and both were still able to deliver electrons from one end to the other, implying the excellent deformability of the network.

The advantages of wavy-configured NW networks could be used to produce dielectric elastomer actuators with enhanced performance. Since the actuators have promising potential as light valves to regulate optical transmittance, they demand effective stretchable transparent electrodes.[21,46] As illustrated in Fig. 5a, dielectric elastomer actuators expand from and contract to their initial state according to the applied voltages. Their compliant electrodes, therefore, should endure repeated mechanical deformation. Since wavy-configured NW networks can satisfy this requirement, their use in compliant electrodes is expected to improve the performance of dielectric elastomer actuators. The performance is characterized by the change in area under an applied voltage, which is quantified as the expansion ratio (A/A_0, where A and A_0 are the area of the actuator with and without the applied voltage, respectively).

The NW networks were transferred onto both sides of a dielectric elastomer (VHB 4905) and their actuation was investigated by applying alternating-current voltages (0.2 Hz). As shown in Fig. 5b, the wavy-configured NW network functioned as a compliant electrode in the dielectric elastomer actuator. We also confirmed that the optical transmittance of the actuator could be controlled by the voltage applied. The transmittance spectra of the actuator in the wavelength range from 350 to 800 nm are provided in Fig. S9†. Fig. 5c shows the expansion ratios of actuators incorporating wavy-configured or uncompressed NW networks as a function of the applied voltages. Under low applied voltages (less than 2 kV), both actuators exhibited identical behaviors: a larger expansion ratio at a larger applied voltage. However, as the applied voltage increased, the expansion ratio of the actuator with a

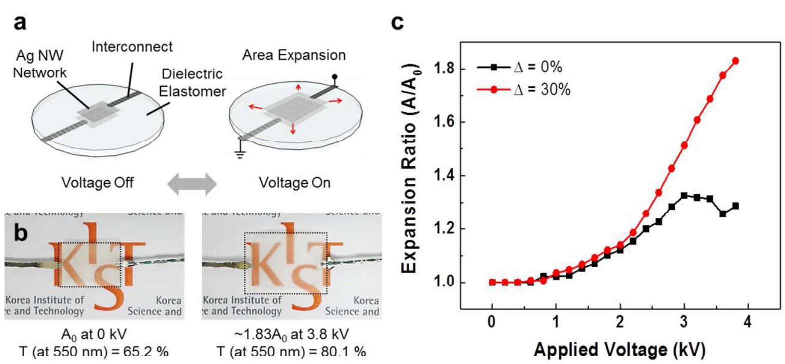

Fig. 5 (a) Schematic diagram of dielectric elastomer actuators employing Ag NW networks as compliant electrodes. (b) Photographs of the actual actuator incorporating a wavy-configured Ag NW network. With no voltage applied, the initial area (A_0) of the actuator was ~25 × 17.5 mm^2 and the transmittance at 550 nm was 65.2%. At 3.8 kV, the area increased to ~1.83A_0 and the transmittance at 550 nm increased to 80.1%. (c) Variation in the area of actuators as a function of the applied voltage. Two actuators were prepared using NW networks with degrees of compression (Δ) of 0% and 30%.

wavy-configured NW network increased continuously up to 3.8 kV, whereas that of the actuator with an uncompressed NW network began to decline at 3 kV. As a result, the maximum expansion ratio of the former was 1.83, which was much larger than that of the latter (1.33). The expansion ratios obtained using actuators incorporating wavy-configured NW networks were larger than those obtained using straight Ag NW networks with even higher population of NWs.[46]

Conclusions

We have demonstrated that manipulating the configuration of Ag NW networks offers key benefits in application of stretchable transparent electrodes. Through compressing Ag NW networks that is initially floated on water and subsequent transferring, Ag NW networks with wavy configurations can easily be prepared and deposited on desired substrates. The resulting NW networks show desirable optical and electrical property as well as greatly enhanced electromechanical stability. As demonstrated in their application to dielectric elastomer actuators, Ag NW networks with wavy configurations allow the fabrication of soft electronic devices with improved performance.

Experimental

Preparation of Ag NW networks with wavy configurations.

A solution containing Ag NWs with an average diameter of ~115 nm and an average length of ~40 μm was purchased from Seashell Technology (AgNW-115). The concentration of Ag NW dispersion was regulated by mixing with ethanol to control the area density of NWs in the networks. The optimized area density was ~0.066 μg/mm^2, which can provide high transparency as well as wavy structure for the networks. A Ag NW network was prepared by vacuum filtration of the solution through an anodized aluminum oxide (AAO) membrane (Whatman, WHA68095012). The NW network on the AAO membrane was peeled off by dipping gently into water, offering the NW network floated on water. To develop a wavy configuration, the NW network with a size of 25 × 25 mm^2 was uniaxially compressed. The compressed length was adjusted to be the 10%, 20%, or 30% of the initial length to control the waviness of the NW network. The resulting NW network was transferred to various target substrates such as PDMS, PET, glass, rubber, and paper by vertical contact from the air. Then, the NW networks on the substrates were dried at 60 °C for 30 min. PDMS (Dow Corning, Sylgard 184), in particular, was utilized as a substrate for the characterization of electrodes (transmittance, sheet resistance, strain tests, and cycle tests). The PDMS substrate was prepared by mixing prepolymer and curing agent in a 10 : 1 weight ratio and following curing at 60 °C for 4 h.

Characterization of Ag NW networks.

The morphology of Ag NW networks was observed with an optical microscope (Leica, DM 2500M). The waviness of NW networks was calculated by using the equation (1) with the contour length (L_c) and the end-to-end distance (L_0) of NWs measured from the acquired images. Square grids of 25 × 25 μm^2 were drawn on the images to determine L_c and L_0 with image processing software (National Institute of Health, Image J). NWs crossing at least two edges of a square grid were chosen for the measurement. The average degree of waviness (W_{avg}) for each NW network was determined by averaging W of 50 NWs from 5 different acquired images. The optical transmittance was measured with an UV-Vis-NIR spectrometer (Jasco, V-600). The sheet resistance was measured at room temperature by a standard four-point probe meter (Napson, CRESBOX). The strain tests were conducted using the in-house strain equipment connected to a multimeter (Fluke, 87V). Eutectic gallium-indium (Sigma Aldrich) was applied at the edge of the NW network to reduce contact resistance.

Fabrication and characterization of dielectric elastomer actuators.

Acrylic elastomer films (3M, VHB 4905) were pre-strained to 300%. After controlling the configuration of the NW networks floated on water, they were transferred to both sides of pre-strained elastomer films. Eutectic gallium-indium was employed as interconnect. A function generator (Agilent, 33250A) and a voltage amplifier (Matsusada Precision Inc., AMT-10B10) were utilized to control the applied voltage to the actuators. The performance of the actuators was observed under an alternating-current voltage in the range of 0 to 3.8 kV that is in the form of a step wave at a frequency of 0.2 Hz.

Acknowledgements

This work was supported by a grant (code no. 2011-0032156) from the Center for Advanced Soft Electronics under the Global Frontier Research Program of the Ministry of Science, ICT & Future Planning, and Republic of Korea. We also acknowledge the financial support from the R&D Convergence Program of National Research Council of Science and Technology of Republic of Korea and a Korea Institute of Science and Technology internal project. S.-S. Lee appreciates the research grant from the KU-KIST Graduate School.

References

1 J. A. Rogers, T. Someya and Y. Huang, *Science*, 2010, **327**, 1603–1607.
2 T. Sekitani, Y. Noguchi, K. Hata, T. Fukushima, T. Aida and T. Someya, *Science*, 2008, **321**, 1468–1472.
3 D. Son, J. Lee, S. Qiao, R. Ghaffari, J. Kim, J. E. Lee, C. Song, S. J. Kim, D. J. Lee, S. W. Jun, S. Yang, M. Park, J. Shin, K. Do, M. Lee, K. Kang, C. S. Hwang, N. Lu, T. Hyeon and D.-H. Kim, *Nat. Nanotechnol.*, 2014, **9**, 397–404.
4 J. Lee, P. Lee, H. B. Lee, S. Hong, I. Lee, J. Yeo, S. S. Lee, T. S. Kim, D. Lee and S. H. Ko, *Adv. Funct. Mater.*, 2013, **23**, 4171–4176.
5 A. R. Madaria, A. Kumar and C. Zhou, *Nanotechnology*, 2011, **22**, 245201.
6 J. Viventi, D.-H. Kim, L. Vigeland, E. S. Frechette, J. A. Blanco, Y.-S. Kim, A. E. Avrin, V. R. Tiruvadi, S.-W. Hwang, A. C. Vanleer, D. F. Wulsin, K. Davis, C. E. Gelber, L. Palmer, J. Van

der Spiegel, J. Wu, J. Xiao, Y. Huang, D. Contreras, J. A. Rogers and B. Litt, *Nat. Neurosci.*, 2011, **14**, 1599–1605.
7 D.-H. Kim, J. Viventi, J. J. Amsden, J. Xiao, L. Vigeland, Y.-S. Kim, J. A. Blanco, B. Panilaitis, E. S. Frechette, D. Contreras, D. L. Kaplan, F. G. Omenetto, Y. Huang, K.-C. Hwang, M. R. Zakin, B. Litt and J. A. Rogers, *Nat. Mater.*, 2010, **9**, 511–517.
8 S. Jung, J. H. Kim, J. Kim, S. Choi, J. Lee, I. Park, T. Hyeon and D. H. Kim, *Adv. Mater.*, 2014, **26**, 4825–4830.
9 M. Amjadi, A. Pichitpajongkit, S. Lee, S. Ryu and I. Park, *ACS Nano*, 2014, **8**, 5154–5163.
10 Y. H. Kim, C. Sachse, M. L. MacHala, C. May, L. Müller-Meskamp and K. Leo, *Adv. Funct. Mater.*, 2011, **21**, 1076–1081.
11 S. Nambiar and J. T. W. Yeow, *Biosens. Bioelectron.*, 2011, **26**, 1825–1832.
12 S.-I. Na, S.-S. Kim, J. Jo and D.-Y. Kim, *Adv. Mater.*, 2008, **20**, 4061–4067.
13 S. Ahn, A. Choe, J. Park, H. Kim, J. G. Son, S.-S. Lee, M. Park and H. Ko, *J. Mater. Chem. C*, 2015, **3**, 2319–2325.
14 J. Zang, C. Cao, Y. Feng, J. Liu and X. Zhao, *Sci. Rep.*, 2014, **4**, 06492.
15 X. Wang, L. Zhi and K. Müllen, *Nano Lett.*, 2008, **8**, 323–327.
16 S. Han, S. Hong, J. Ham, J. Yeo, J. Lee, B. Kang, P. Lee, J. Kwon, S. S. Lee, M.-Y. Yang and S. H. Ko, *Adv. Mater.*, 2014, **26**, 5808–5814.
17 P. Lee, J. Lee, H. Lee, J. Yeo, S. Hong, K. H. Nam, D. Lee, S. S. Lee and S. H. Ko, *Adv. Mater.*, 2012, **24**, 3326–3332.
18 L. Hu, H. S. Kim, J. Lee, P. Peumans and Y. Cui, *ACS Nano*, 2010, **4**, 2955–2963.
19 F. Xu and Y. Zhu, *Adv. Mater.*, 2012, **24**, 5117–5122.
20 X. Ho, J. Nie Tey, W. Liu, C. Kweng Cheng and J. Wei, *J. Appl. Phys.*, 2013, **113**, 044311.
21 J. Wu, J. Zang, A. R. Rathmell, X. Zhao and B. J. Wiley, *Nano Lett.*, 2013, **13**, 2381–2386.
22 C. Yang, H. Gu, W. Lin, M. M. Yuen, C. P. Wong, M. Xiong and B. Gao, *Adv. Mater.*, 2011, **23**, 3052–3056.
23 M. Nogi, N. Komoda, K. Otsuka and K. Suganuma, *Nanoscale*, 2013, **5**, 4395–4399.
24 L. Cai, J. Li, P. Luan, H. Dong, D. Zhao, Q. Zhang, X. Zhang, M. Tu, Q. Zeng, W. Zhou and S. Xie, *Adv. Funct. Mater.*, 2012, **22**, 5238–5244.
25 Y. Zhu and F. Xu, *Adv. Mater.*, 2012, **24**, 1073–1077.
26 T. Chen, Y. Xue, A. K. Roy and L. Dai, *ACS Nano*, 2014, **8**, 1039–1046.
27 D.-S. Leem, A. Edwards, M. Faist, J. Nelson, D. D. C. Bradley and J. C. de Mello, *Adv. Mater.*, 2011, **23**, 4371–4375.
28 V. Scardaci, R. Coull, P. E. Lyons, D. Rickard and J. N. Coleman, *Small*, 2011, **7**, 2621–2628.
29 D. Lee, H. Lee, Y. Ahn and Y. Lee, *Carbon*, 2015, **81**, 439–446.
30 Y. Zhu, Q. Qin, F. Xu, F. Fan, Y. Ding, T. Zhang, B. J. Wiley and Z. L. Wang, *Phys. Rev. B: Condens. Matter Mater. Phys.*, 2012, **85**, 045443.
31 H.-L. Gao, L. Xu, F. Long, Z. Pan, Y.-X. Du, Y. Lu, J. Ge and S.-H. Yu, *Angew. Chem.*, 2014, **53**, 4561–4566.
32 J. Ge, H.-B. Yao, X. Wang, Y.-D. Ye, J.-L. Wang, Z.-Y. Wu, J.-W. Liu, F.-J. Fan, H.-L. Gao, C.-L. Zhang and S.-H. Yu, *Angew. Chem. Int. Ed.*, 2013, **52**, 1654–1659.
33 L. Song, A. C. Myers, J. J. Adams and Y. Zhu, *ACS Appl. Mater. Interfaces*, 2014, **6**, 4248–4253.
34 D. J. Lipomi, M. Vosgueritchian, B. C.-K. Tee, S. L. Hellstrom, J. a. Lee, C. H. Fox and Z. Bao, *Nat. Nanotechnol.*, 2011, **6**, 788–792.
35 F. Xu, J. W. Durham, B. J. Wiley and Y. Zhu, *ACS Nano*, 2011, **5**, 1556–1563.
36 F. Xu, W. Lu and Y. Zhu, *ACS Nano*, 2011, **5**, 672–678.
37 D.-H. Kim, R. Ghaffari, N. Lu and J. A. Rogers, *Annu. Rev. Biomed. Eng.*, 2012, **14**, 113–128.
38 B. Wu, A. Heidelberg, J. J. Boland, J. E. Sader, X. Sun and Y. Li, *Nano Lett.*, 2006, **6**, 468–472.
39 J. Huang, M. Juszkiewicz, W. H. de Jeu, E. Cerda, T. Emrick, N. Menon, T. P. Russell, E. Kesselman, Y. Talmon, M. A. Hillmyer, T. P. Lodge, F. S. Bates, J. Huang, M. Juszkiewicz, W. H. de Jeu, E. Cerda, T. Emrick, N. Menon and T. P. Russell, *Science*, 2007, **317**, 650–653.
40 C. F. Guo, T. Sun, Q. Liu, Z. Suo and Z. Ren, *Nat. Commun.*, 2014, **5**, 3121.
41 J. Wang, C. Yan, W. Kang and P. S. Lee, *Nanoscale*, 2014, **6**, 10734–10739.
42 D. L. Simonato, G. Giusti, C. Mayousse, C. Celle, D. Bellet and Jean-Pierre, *Nanotechnology*, 2013, **24**, 452001.
43 S. De, T. M. Higgins, P. E. Lyons, E. M. Doherty, P. N. Nirmalraj, W. J. Blau, J. J. Boland and J. N. Coleman, *ACS Nano*, 2009, **3**, 1767–1774.
44 J. Y. Woo, K. K. Kim, J. Lee, J. T. Kim and C.-S. Han, *Nanotechnology*, 2014, **25**, 285203.
45 J. Lee, I. Lee, T. Kim and J. Lee, *Small*, 2013, **9**, 2887–2894.
46 S. Shian, R. M. Diebold, A. McNamara and D. R. Clarke, *Appl. Phys. Lett.*, 2012, **101**, 061101.